



Impacts of ground-level ozone on sugarcane production

Alexander W. Cheesman^{a,b,*}, Flossie Brown^b, Mst Nahid Farha^{a,c}, Thais M. Rosan^b, Gerd A. Folberth^d, Felicity Hayes^e, Barbara B. Moura^{f,g}, Elena Paoletti^{f,h}, Yasutomo Hoshika^{f,h}, Colin P. Osborneⁱ, Lucas A. Cernusak^a, Rafael V. Ribeiro^j, Stephen Sitch^b

^a College of Science & Engineering and Centre for Tropical Environmental and Sustainability Science, James Cook University, Cairns, Queensland, Australia

^b Faculty of Environment, Science and Economy, University of Exeter, Exeter, UK

^c Department of Chemistry, Rajshahi University of Engineering & Technology, Rajshahi 6204, Bangladesh

^d UK Met Office Hadley Centre, Exeter, UK

^e UK Centre for Ecology & Hydrology, Environment Centre Wales, Bangor, Gwynedd LL57 2UW, UK

^f Institute of Research on Terrestrial Ecosystems (IRET), National Research Council of Italy (CNR), Sesto Fiorentino, Italy

^g NBFC, National Biodiversity Future Center, Palermo 90133, Italy

^h Italian Integrated Environmental Research Infrastructures System (ITINERIS), Tito Scalco, 85050 Potenza, Italy

ⁱ Plants, Photosynthesis and Soil, School of Biosciences, University of Sheffield, Sheffield, UK

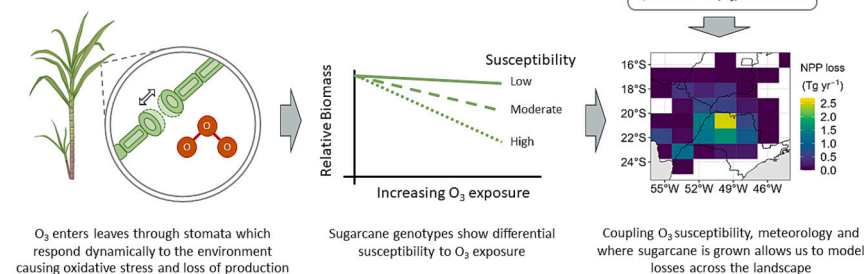
^j Laboratory of Crop Physiology (LCroP), Department of Plant Biology, Institute of Biology, University of Campinas (UNICAMP), Campinas, SP, Brazil

HIGHLIGHTS

- Sugarcane is a commodity crop grown across the (sub)tropics.
- Ozone exposure causes a reduction in productivity of sugarcane.
- Cultivars of sugarcane show different sensitivities to ozone.
- Spatial modelling shows variation in the risks of O₃ across south-central Brazil.
- Ozone poses a substantial production risk for the world's largest regional producer.

GRAPHICAL ABSTRACT

Impacts of ozone (O₃) on sugarcane production



ARTICLE INFO

Editor: Jay Gan

Keywords:
Bioenergy
Tropospheric
O₃
JULES
Air pollution
Brazil

ABSTRACT

Sugarcane is a vital commodity crop often grown in (sub)tropical regions which have been experiencing a recent deterioration in air quality. Unlike for other commodity crops, the risk of air pollution, specifically ozone (O₃), to this C₄ crop has not yet been quantified. Yet, recent work has highlighted both the potential risks of O₃ to C₄ bioenergy crops, and the emergence of O₃ exposure across the tropics as a vital factor determining global food security. Given the large extent, and planned expansion of sugarcane production in places like Brazil to meet global demand for biofuels, there is a pressing need to characterize the risk of O₃ to the industry. In this study, we sought to a) derive sugarcane O₃ dose-response functions across a range of realistic O₃ exposure and b) model the implications of this across a globally important production area. We found a significant impact of O₃ on biomass allocation (especially to leaves) and production across a range of sugarcane genotypes, including two

* Corresponding author at: College of Science & Engineering and Centre for Tropical Environmental and Sustainability Science, James Cook University, Cairns, Queensland, Australia.

E-mail address: Alexander.Cheesman@gmail.com (A.W. Cheesman).

<https://doi.org/10.1016/j.scitotenv.2023.166817>

Received 3 July 2023; Received in revised form 27 August 2023; Accepted 2 September 2023

Available online 4 September 2023

0048-9697/© 2023 The Authors. Published by Elsevier B.V. This is an open access article under the CC BY license (<http://creativecommons.org/licenses/by/4.0/>).

commercially relevant varieties (e.g. CTC4, Q240). Using these data, we calculated dose-response functions for sugarcane and combined them with hourly O_3 exposure across south-central Brazil derived from the UK Earth System Model (UKESM1) to simulate the current regional impact of O_3 on sugarcane production using a dynamic global vegetation model (JULES v1.5.6). We found that between 5.6 % and 18.3 % of total crop productivity is likely lost across the region due to the direct impacts of current O_3 exposure. However, impacts depended critically on the substantial differences in O_3 susceptibility observed among sugarcane genotypes and how these were implemented in the model. Our work highlights not only the urgent need to fully elucidate the impacts of O_3 in this important bioenergetic crop, but the potential implications air quality may have upon tropical food production more generally.

1. Introduction

1.1. Sugarcane

Sugarcane is the common name given to a diverse group of cultivated, sucrose-storing, tropical grasses that are an important food and commodity crop to many countries (Moore et al., 2014) and the source of ~80 % of world's sugar (FAOSTAT, 2021). Brazil is the world's largest producer of sugarcane, with approximately 99,706 km² given over to sugarcane production, resulting in 36.4 % of global output (i.e. 716 million tonnes), as compared to the second largest producer India at 405 million tonnes (20.5 % of global output) (FAOSTAT, 2021). The dominance of Brazil in sugarcane production has come about in part due to improved technologies and breeding programs, but in the main due to the rapid expansion in cultivated area over the last 20 years (Ogura et al., 2022), with production focused in south-central Brazil (Zheng et al., 2022). The state of São Paulo alone accounts for ~47 % of Brazil's total sugarcane production (Ogura et al., 2022) with the three next largest state producers (Goiás, Minas Gerais, and Mato Grosso do Sul) all in the south-central region (Fig. 1) and showing recent rapid expansion (Zalles et al., 2019). Brazil recognizes sugarcane as its third most valuable crop in terms of gross value (IBGE, 2023), supplying raw material for sugar, ethanol (biofuel), and direct energy production. Indeed sugarcane-derived products account for ~16.4 % of the Brazilian energy matrix (EPE, 2023). Sugarcane therefore contributes substantially to the bioeconomy of both Brazil and the state of São Paulo specifically (Ogura et al., 2022), and with increasing global demand for fossil fuel alternatives and the development of next generation biorefineries, a continued

expansion of this industry is likely in the coming years (Vandenbergh et al., 2022).

The recent rapid expansion of commodity crops such as sugarcane in Brazil has resulted in both the repurposing of existing C₄ grass dominated pasturelands and the conversion of natural vegetation, including both Amazon humid tropical forests and Cerrado dry tropical savannas (Ogura et al., 2022; Zalles et al., 2019). The resulting tension between the production of 'green fuels' at the cost of existing natural systems requires that steps are taken to maximise productivity of existing and planned sugarcane agricultural areas (Rossetto et al., 2022; Spera, 2017).

1.2. O_3 impacts on vegetation

At the Earth's surface, ozone (O_3) is considered a major atmospheric pollutant, posing a risk to both human health and plant growth (Lelieveld et al., 2015; Mills et al., 2018a). Indeed the impact of O_3 on agro-nomic productivity has been appreciated since the early observation of 'oxidative stipple' in grape vines (Richards et al., 1958). The " O_3 -yield gap" recognized in many temperate and commodity crop species (Ainsworth, 2017; Mills et al., 2007) results in an estimated global productivity loss of 12.4 %, 7.1 %, 4.4 % and 6.1 % for soybean, wheat, rice and maize, respectively (Mills et al., 2018b). Recognition of the impacts of O_3 on both agronomic and natural systems, as well as the direct implications on human health, has resulted in air quality control treaties across many mid-latitude countries. Treaties such as the UNECE's Long-range Transboundary Air Pollution (LRTAP) Convention and the resulting Task Force on Hemispheric Transport of Air Pollution (TF

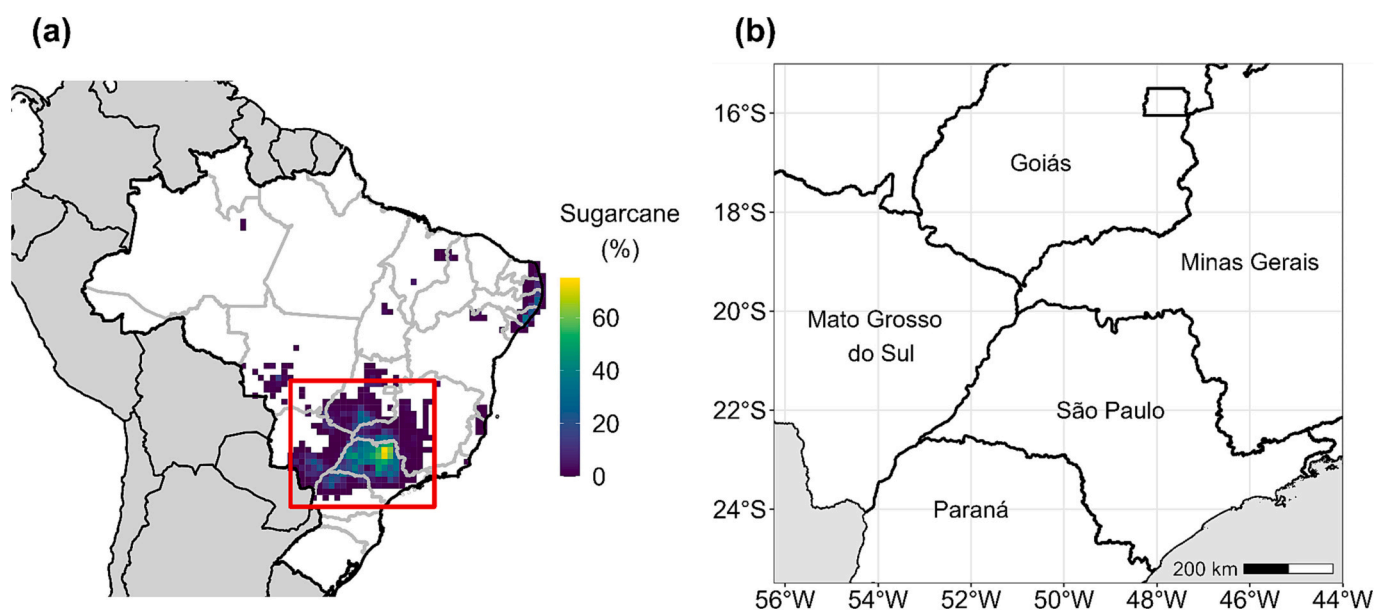


Fig. 1. Percentage of land cover dedicated to sugarcane production across Brazil in year 2020 (a) and modelling extent in south-central Brazil (b). Sugarcane coverage data from MapBiomass v6 (www.plataforma.brasil.mapbiomass.org) see Souza et al. (2020) for details, plotted here with a spatial resolution of 0.5°. Note map lines delineate general study area in South America and does not necessarily depict accepted national boundaries.

HTAP, www.htap.org) that have helped to reduce O₃ or at least stabilize ambient O₃ levels across much of the global north (Doherty, 2015; Mills et al., 2018a).

1.3. Air quality and O₃ exposure in Brazil

Unlike countries in the global north, much of the (sub)tropics is seeing the continuing expansion of O₃ precursor emissions (especially NO_x); from population growth, urbanization, biomass burning associated with land conversion, and the rise in large-scale agro-industry (Granier et al., 2000; Hewitt et al., 2009). When coupled to high temperatures and generally high levels of volatile organic compounds (VOCs) emitted by tropical vegetation, it is likely that O₃ responsiveness will emerge as a significant factor in limiting tropical crop yields and quality in the coming decades (Hayes et al., 2020; Tai et al., 2014).

In Brazil levels of O₃ are generally high, with large episodic events associated with vehicle exhaust in metropolitan areas (Schuch et al., 2019), biomass burning, and regional atmospheric drought (Targino et al., 2019). Historically, the controlled pre-harvest burning of sugarcane was itself responsible for considerable O₃ precursor emissions (Urban et al., 2016). However, this has been reduced by the industry's adoption of mechanization, in part due to efforts such as the "Green Ethanol" protocol, a voluntary standard established in response to São Paulo State Law number 11,241 banning the practice of pre-harvest burning (on lands with a low topographic gradient) by 2021 (ALESP, 2002). Yet, the waste sugarcane biomass (bagasse) is still often burnt for direct energy production in industrial plants which, given the trans-boundary movement of O₃ and its precursors (e.g. NO_x), can still result in reduced air quality across rural areas (Squizzato et al., 2021).

Regions of poor air quality (including high O₃) around south-central Brazil have been noted as having an impact on native vegetation (Moura et al., 2018a), and are projected to deteriorate further in the coming decades, both in response to continued precursor emissions from expanding megacities (Folberth et al., 2015), and due to changes in atmospheric chemistry in a warmer world (Brown et al., 2022). Given this trajectory, there is a need to consider how the magnitude of O₃ damage to sugarcane may vary across south-central Brazil in order to support a sustainable expansion of the industry (Rossetto et al., 2022).

1.4. Impact of O₃ on sugarcane

Sugarcane and related C₄ grass species have a biophysical CO₂ concentrating mechanism (Sage et al., 2014), resulting in high light, nitrogen, and water use efficiencies (i.e. carbon fixed per unit water lost) under warm-climatic conditions (Rao and Dixon, 2016). Given their inherent high water use efficiency, it is often presumed that C₄ grasses may avoid the deleterious effects of O₃ via stomatal exclusion; or that, by evolving effective antioxidant capacity to deal with climate induced oxidative stress, they may be well placed to deal with the reactive oxygen species formed by exposure to O₃ (Grantz and Vu, 2009). Certainly, in the early examination of C₄ grasses, it appeared that they showed only limited impacts of O₃ fumigation (Volin et al., 1998). However, from a recent broad examination of O₃ susceptibility in C₄ bioenergy crops by Li et al. (2022) it is clear that a high degree of variability exists, with initial studies indicating sugarcane itself to be highly susceptible to O₃ (Grantz and Vu, 2009; Grantz et al., 2012; Moura et al., 2018b). Yet despite this, it is notable that the only attempts to date to model the implications of sugarcane's O₃ susceptibility have been parameterized using the response of the C₃ crop cotton (*Gossypium hirsutum*) (Chuwah et al., 2015; Yi et al., 2018).

Commercial sugarcane cultivars are complex interspecific hybrids, primarily between *Saccharum officinarum*, known as the noble cane, and *S. spontaneum*, with contributions from *S. robustum*, *S. sinense*, *S. barberi*, and related grass genera such as *Miscanthus*, *Narenga*, and *Erianthus* (Moore et al., 2014). Domesticated sweet chewing cane *S. officinarum* was often hybridised with lines of *S. spontaneum* to confer reduced

susceptibility to abiotic and biotic stress, improved vegetative vigour, and to enhance traits beneficial to mechanized harvesting and processing. Although screening for O₃ tolerance is not currently a key trait in breeding programs, Grantz et al. (2012) demonstrated that the degree of photosynthetic inhibition seen under O₃ fumigation was inversely proportional to the contribution of *S. spontaneum* germplasm to the hybrid genome of four genetic lines. Similarly, it is well established that there are differences across modern sugarcane cultivars in traits, such as antioxidant capacity (Boaretto et al., 2014; Moura et al., 2018c) and intrinsic water use efficiency (Basnayake et al., 2015; Natarajan et al., 2021), that may well determine cultivar specific responses to O₃ (Wedow et al., 2021).

Given the current extent, and planned expansion of sugarcane production to meet global demand for 'green' biofuels across the world, there is a pressing need to characterize the potential risk of current O₃ exposure to the sugarcane industry. We therefore sought to: a) derive sugarcane O₃ dose-response functions across a full range of O₃ exposure; and b) model the implications of observed sugarcane susceptibility to O₃ across the globally important production area of south-central Brazil. Our findings will not only have direct implications on the world's primary sugarcane producing region, but will also inform global efforts to identify and address the O₃ yield gap under future climate and land use change scenarios.

2. Materials and methods

2.1. Experimental facility

All O₃ exposure studies were conducted at the joint University of Exeter (UoE) and James Cook University (JCU) TropOz research facility (www.tropoz.org) located on the Nguma-bada campus of JCU in Cairns, Queensland, Australia. This unique tropical facility allows for the study of O₃ responses of plants grown under ambient tropical humid conditions, and consists of nine independently controlled and monitored Open Top Chambers (OTCs). Each chamber (internal volume 22.2 m³) was ventilated with charcoal filtered air at ~2 m³ s⁻¹ using separate inline square centrifugal fans (ICQ560-VEE, Pacific Ventilation, Melbourne, VIC) augmented with O₃ generated on site and supplied to each chamber between 8:00 and 17:00. A different level of O₃ was applied to each individual chamber to achieve a semi-continuous gradient of nine different O₃ exposures (average chamber daytime concentrations ranged between 15 and 120 ppb, Table A1). This gradient-design provides a better approach than replicating a small number of exposure points, when seeking to identify a potentially nonlinear treatment response (Kreyling et al., 2018). Ozone concentrations in each chamber were monitored sequentially using an ultraviolet (UV) absorption O₃ analyser (Model 205, 2B technology, Boulder CO, USA) in air brought to a centralized service hub via a vacuum pump (Labport 840FT.18, KNF, Moreland West, VIC, Australia). A typical sampling sequence was achieved every 22 min allowing approximately three O₃ concentration readings per hour per chamber. Environmental variables including air temperature (T), vapour pressure deficit (VPD), and photosynthetically active radiation (PAR) were monitored using a single meteorological monitoring station (Campbell Scientific, Logan UT, USA) established in the central OTC and recording data averaged over every five minutes (Table A2).

2.2. Plant material

To develop O₃ dose-response functions for sugarcane, four *Saccharum* genetic lines were selected: *Saccharum officinarum* L. cv. Badila, a 'noble cane' often grown commercially in the early 20th Century and commonly used as the basis for breeding programs; *Saccharum spontaneum* cv. Mandalay, a clone used historically in Australian sugarcane breeding programs; and two commonly used commercial hybrid lines Q240 – which although being released in 2009 by Sugar Research

Australia (SRA) still dominates (~40 %) Australian (Queensland) sugarcane plantings, and CTC4 which represented around 10 % of 2019/20 plantings in the main producing areas of Brazil (Braga Junior et al., 2021).

Cane material held at the SRA germplasm collection (Meringa, Queensland, Australia) was supplied by SRA under licence in October 2021. This material was used to derive ~60 one-eye sets from each genetic line, which were treated with a systemic fungicide (Tilt 500 EC, Syngenta Australia, active constituent Propiconazole) and set to germinate under ambient shadehouse conditions at JCU's Environmental Research Complex (www.jcu.edu.au/environmental-research-complex). After one month an even cohort of sugarcane starts from each line were set out into individual 30-L pots containing a high organic matter potting mix augmented with a volcanic stone Quinkan to improve drainage. After establishment of the plants, all pots were maintained at close to field capacity with daily dripline irrigation, and fertilized every two weeks using Peters Professional Blossom Booster (10–13–16 + 1.2 Mg + TE, ICL Australia, Bella Vista, NSW, Australia).

For the determination of O₃ dose-response functions, four individuals of each genetic line were placed into each of the nine OTCs. Three of the varieties (Badila, Q240 and CTC4) were moved to the OTCs when ~10 cm tall on 13 November 2021 to begin the O₃ exposure experiment (duration 96 days). However, given initial slow growth, Mandalay was delayed and placed into the OTC on 28 March 2022 to begin its 100-day exposure. As a result of this delay different environmental conditions were experienced during the two experimental runs (Table A2); however, in both cases plants experienced full-sunlight and were not subjected to drought. Any residual differences in environmental conditions experienced between the two experimental runs should be accounted for in the calculation of O₃ flux dose-response functions (see Section 2.3).

2.3. Characterizing O₃ dose-response functions of sugarcane biomass

At the conclusion of the experiment, plants were harvested and oven dried (70 °C) until constant mass to determine biomass production. Biomass was partitioned into: leaf (all photosynthetic material distal from leaf ligules), stalks (including cane and leaf sheath), and roots. At this stage, the most recently emerged leaf after ligule separation (L + 1) from each plant was collected separately to determine individual leaf area, dry biomass and thereby leaf mass per area (LMA).

In addition to relating changes in biomass to the concentration-based O₃ exposure metric AOT40 (ppm.h), we estimated accumulated O₃ flux into leaves using the Deposition of O₃ for Stomatal Exchange (DO₃SE) model v3.1. The use of DO₃SE to calculate the Phytotoxic Ozone Dose (POD_y, mmol m⁻², above a threshold y in nmol O₃ m⁻² projected leaf area (PLA) s⁻¹) provides for an O₃ metric that accounts for differences in stomatal conductance as a result of species-level traits and environmentally dynamic conditions. Using flux-based metrics allows for the comparison of O₃ susceptibilities collected under diverse environmental conditions and facilitates the linking of observed susceptibility to dynamic vegetation models. Dynamic models which integrate vegetation responses to multiple environmental factors such as soil moisture and temperature to determine O₃ flux (Emberson, 2020; Pleijel et al., 2022).

We modelled stomatal conductance in DO₃SE using an empirically derived model (Jarvis, 1976; Emberson et al., 2000). In the weeks prior to harvest, stomatal conductance to water vapour (g_s) was measured on both the abaxial and adaxial surfaces of L + 1 leaves of all plants from CTC4, Q240 and Badila using a handheld porometer (SC1, Decagon Devices, Pullman WA, USA). As porometer data could not be collected on Mandalay, given its narrow leaf blade, and the fact we observed no significant decline in g_s of sunlit (PAR > 1500 $\mu\text{mol m}^{-2} \text{s}^{-1}$) L + 1 leaves as measured using the porometer across O₃ exposure, we also collected data from the control chamber plants of all genotypes using a portable photosynthesis analyser (LI-6400XT, LiCOR Biosciences, Lincoln NE, USA). This leaf-level gas-exchange data comprised survey

measurements collected every three minutes for ~24 h per leaf using a buffer volume and with the LI-6400xt tracking ambient PAR and temperatures. All g_s data were converted to Relative Stomatal Conductance (RSC) before fitting DO₃SE Jarvis parameters (Tables 1 and A3) using the method described by Hayes et al. (2020a), with stomatal conductance of O₃ (g_{o3}) = 0.663 × g_s . The ability of the DO₃SE model to represent g_s in sugarcane was verified by comparing modelled values with those measured using the LI-6400xt (Fig. A1). All genotypes showed a strong positive correlation between observed and modelled daylight (i.e. 5:30 to 19:00) data with an R² ranging from 0.59 in CTC4 to 0.83 in Mandalay.

The O₃ flux-based metric POD_y was calculated for each genotype-chamber combination using the DO₃SE model calibrated using gas exchange data (Table 1) and y -values 0 to 8 nmol m⁻² s⁻¹. The y -value represents an instantaneous O₃ flux below which no damage due to O₃ is assumed to occur, and is considered reflective of plants' resistance to O₃ (Agathokleous and Saitanis, 2020). We selected two thresholds (i.e. 0 and 2 nmol m⁻² s⁻¹) to use in the regional simulations (see Section 2.4); the use of POD₀ did not presuppose the same inherent resistance across sugarcane genotypes (Agathokleous et al., 2019), whereas POD₂ allowed for comparison with previously published O₃ dose-response functions (Moura et al., 2018b). Dose-response functions were calculated for the relative biomass decline using a maximum biomass estimated as the y -intercept of a linear regression between average total biomass ($n = 4$) of each chamber ($n = 9$) and the calculated POD_y.

2.4. Modelling impacts of O₃ exposure in south-central Brazil

To model the potential risks of current O₃ levels to sugarcane production across south-central Brazil, we used the Joint UK Land Environment Simulator (JULES) (Best et al., 2011; Clark et al., 2011) v5.6. JULES is a land surface model used to study soil-vegetation-atmosphere interactions in which the land is divided into gridcells and vegetation is represented by up to 13 plant functional types (PFTs). Outputs are given as an average for each gridcell assuming homogeneity within the gridcell, and each PFT represents the average behaviour of that vegetation type based on observations (Harper et al., 2016). Sugarcane is a C₄ crop so here we focused only on the C₄ PFT, with modifications made to better represent sugarcane (see Section 2.4.1). Each gridcell can contain a mixture of PFTs and non-vegetation cover, and we prescribed the fraction of the C₄ PFT in each gridcell to match the observed distribution of sugarcane across south-central Brazil (see Section 2.4.5).

This modelling framework incorporates continuous and spatially explicit environmental information (e.g. meteorological conditions and [O₃]) and calculates vegetation responses and fluxes in each gridcell, taking into account soil properties and vegetation processes, including photosynthesis, respiration, and carbon partitioning for each PFT. JULES outputs information at the gridcell scale, rather than at the individual plant scale, and therefore differs from some detailed crop models by not including management decisions such as harvesting and ratooning. However, the model has substantial complexity including the representation of vegetation responses to atmospheric composition, e.g. CO₂ (Huntingford et al., 2013), aerosols (Mercado et al., 2009; Rap et al., 2018), and O₃ (Leung et al., 2022), as well as interaction with other abiotic factors such as temperature (Huntingford et al., 2017), drought (Harper et al., 2021), and changes in nutrient cycling (Huntingford et al., 2022). The model is regularly updated to incorporate new process understanding and additional observations, and the specific model set-up used here is described in more detail in Section 2.4.1.

2.4.1. Details on JULES environment and parameterization

Sugarcane was represented in JULES by using the C₄ PFT. However, to better represent carbon fixation, respiration and stomatal conductance of sugarcane, we used PFT parameters adapted by Vianna et al. (2022). The work by Vianna et al. (2022) used field data from 11 sites across Brazil representing four cultivars (RB867515, IACSP95-5000,

Table 1

Genotype specific stomatal conductance parameterization utilized in DO₃SE to calculate Phytotoxic Ozone Dose (POD). $g_{O_3\text{-max}}$ is the maximum stomatal conductance to O₃, f_{min} is the fraction of $g_{O_3\text{-max}}$ at minimum stomatal conductance ($g_{O_3\text{-min}}$). L_d the effective leaf blade width, f_{temp} , f_{PAR} , f_{VPD} are the functions of g_s response to air temperature (T, °C), photosynthetically active radiation at the leaf surface (PAR, $\mu\text{mol m}^{-2} \text{s}^{-1}$), and vapour pressure deficit (VPD, kPa) respectively. Data derived from leaf-level gas exchange using Li-6400XT.

Genotype	$g_{O_3\text{-max}}$	L_d	f_{min}	f_{PAR}	f_{VPD}		f_{temp}		
	($\text{mmol m}^{-2} \text{s}^{-1}$)				VPD _{min}	VPD _{max}	T _{min}	T _{opt}	T _{max}
		(m)	(fraction)	(unitless)	(kPa)	(kPa)	(°C)	(°C)	(°C)
Badila	185	0.05	0.06	0.005	3.5	6.0	21	34	47
CTC4	172	0.05	0.06	0.008	3.8	5.8	24	37	50
Mandalay	245	0.01	0.06	0.004	1.67	6.64	16	31	46
Q240	153	0.05	0.06	0.010	3.5	7.0	20	35	50
IACSP94-2094 ^a	363	0.05	0.06	0.0014	1.93	5.40	15	32	46
IACSP95-5000 ^a	342	0.05	0.06	0.0015	1.60	6.82	13	32	46

^a Data from Moura et al. (2018b).

RB72454, and CTC14) to tune JULES-Crop for its application to sugarcane. Although this modelling framework does not account for genotype explicitly in the selection of fitting parameters (Table A4), when evaluated it was able to reproduce observed GPP ($\text{kg C m}^{-2} \text{yr}^{-1}$) with an $r^2 = 0.78$ and an accuracy metric (d) = 0.92, representing a RMSE of 6.75 Mg ha^{-1} of stalk dry matter (Vianna et al., 2022).

Stomatal conductance (g_s) within JULES is calculated using the Medlyn stomatal conductance model (Medlyn et al., 2011), parameterized using g_1 from Oliver et al. (2022) ($g_1 = 1.62$ for C₄ plants). Photosynthetic rates were calculated using the Collatz photosynthesis model, and O₃ flux calculated as per Oliver et al. (2018). See Appendix A: Supplementary Information for further details. The Collatz model in JULES uses the photosynthesis parameter V_{max} , calibrated by Vianna et al. (2022) based on the top leaf nitrogen concentration (Table A4).

2.4.2. Ozone data

Given a paucity of directly measured O₃ data across much of south-central Brazil (especially in rural sugarcane growing regions), the O₃ exposure data used herein were simulated using the Earth System Model UKESM1 for the period 2000 to 2015. Modelled [O₃] data are available at a monthly resolution representing 0 to 40 m above orography, and at a horizontal resolution of 1.25° latitude by 1.875° longitude. For our work, the monthly mean surface [O₃] was adapted to reflect both the diel cycle and daily variation observed in the region. Specifically, we projected the same daily variation and diel cycle seen at 53 point-locations in the state of São Paulo in 2018 (CETESB, 2022) to every modelled grid cell (see Appendix A: Supplementary Information, and Figs. A2 to A5 for details). This provided the realistic and biologically relevant [O₃] climatology required to drive our model, and notably resulted in an ~40 % increase in annualized flux of O₃ as compared to the use of monthly mean concentrations as given by UKESM1 (Fig. A6).

2.4.3. Calibrating JULES for sugarcane susceptibility to O₃

The O₃ damage scheme employed here in JULES is the same as that in Sitch et al. (2007) (see Eqs. (1), (2), and (3)) and works by modifying net photosynthesis (A_{net}) and stomatal conductance (g_s) by an O₃ damage factor (F). With F defined (Eq. (1)) by a sensitivity parameter (α) and the flux of O₃ above a threshold (y) so that A decreases linearly (Eq. (2)) as O₃ flux increases above the threshold and the rate of decrease depends on the sensitivity parameter. The decrease in A affects the Net Primary productivity (NPP), and the model assumes that a) O₃ damage is instantaneous at the point of uptake and b) results in a coordinated reduction in g_s (Eq. (3)).

$$F = 1 - \alpha \times (\text{Flux O}_3 > y) \quad (1)$$

$$A_{\text{mod}} = A_{\text{net}} \times F \quad (2)$$

$$g_{\text{mod}} = g_s \times F \quad (3)$$

We derived α within the damage scheme using two thresholds of $y = 0$, and 2 $\text{nmol m}^{-2} \text{s}^{-1}$. To do this we calculated the reduction in modelled NPP compared to a simulation with no O₃ damage for each grid cell over a yearlong run of JULES, using a first approximation for α . Iterative adjustment of α was then carried out until the relative NPP loss modelled in each grid cell due to the O₃ flux matched the dose-response functions observed in this study (i.e. Mandalay, combined commercial, and Badila, see Results and Table 3). We also tuned α to fit the observed O₃ dose-response function for two highly susceptible sugarcane varieties (IACSP94-2094 and IACSP95-5000) published by Moura et al. (2018b). This resulted in the development of eight different α functions across four different susceptibilities (e.g. low, moderate, high, and very high) and two thresholds; and was aimed at characterizing the full range of potential O₃ impacts on sugarcane production (Table 3).

2.4.4. JULES model runs

To develop spatially explicit risk maps of potential O₃ impacts on sugarcane production, JULES was used to calculate annual yields with or without consideration of O₃ susceptibility for a 10-year period (after a 20-year model spin up) across south-central Brazil. Meteorological forcing at 6-h intervals for the years 2005 to 2015 was taken from CRUJRA v2.1 reanalysis (Harris et al., 2020; Kobayashi et al., 2015) at a horizontal resolution of 1.25° latitude by 1.875° longitude, whilst O₃ data was supplied as a yearly climatology with hourly variation as described above and in Appendix A Supplementary Information. Spatially explicit model outputs using α calibrated at four levels of susceptibility (i.e. low, moderate, high and very high) and two thresholds (i.e. 0 and 2 $\text{nmol m}^{-2} \text{s}^{-1}$) were compared to the control model output (i.e. with no O₃ damage) to calculate both proportional decline (% of control) and absolute impacts (reduction in NPP; $\text{kg C m}^{-2} \text{yr}^{-1}$).

2.4.5. Scaling of risk to impacts on sugarcane production and conversion to yield

To convert the modelled risk of O₃ across the landscape to potential reductions in regional sugarcane production, we scaled JULES model outputs by the fractional cover of sugarcane found in each grid cell in the year 2020 (Fig. 1). Sugarcane coverage was derived from MapBiomass v6 (www.plataforma.brasil.mapbiomass.org) (see Souza et al. (2020) for details) and resampled at a spatial resolution (i.e. 1.25° latitude by 1.875° longitude) commensurate with a JULES run. Furthermore, to estimate yield losses of fresh cane (Mg ha^{-1}) we converted from JULES output NPP ($\text{kg C m}^{-2} \text{yr}^{-1}$) employing standard assumptions informed by crop modelling of mature sugarcane (Dias and Sentelhas, 2018; Marin et al., 2016; Marin et al., 2015; Souza et al., 2020). Specifically this included assuming fixed carbon content of biomass of 50 %, above ground biomass representing 80 % of total biomass, a harvest index (proportion cane of total above ground biomass production) of 70 %, and a constant dry matter content of 25 %.

2.5. Statistical analysis

All statistical analyses were conducted in R v 4.2.0 (R Core Team, 2022). Our determination of O₃ dose-response functions utilized a gradient design (Kreyling et al., 2018) in which individual chambers represented an un-replicated point on the gradient of O₃ exposure. A linear regression between chamber averaged data for individual plants (n = 4) and O₃ metric (i.e. AOT40, or POD_y) was translated to genotype specific O₃ dose-response functions (i.e. changes in relative biomass) using a maximum biomass estimated as the y-intercept of a linear regression between total biomass and the O₃ metric. When considering morphological impacts of O₃ exposure on sugarcane traits, we fitted a linear mixed effects model to predict, for example LMA, with increasing POD_y and included 'genotype' as a random effect.

3. Results

3.1. O₃ dose-response function of sugarcane

Sugarcane genotypes grown as part of this study showed significant differences in growth over the ~100 day experimental period (Table 2, Fig. 2a). The two commercial varieties (i.e. CTC4, Q240) produced substantially more biomass than either the *S. officinarum* cv. Badila or *S. spontaneum* cv. Mandalay, with Mandalay having the lowest final biomass under low [O₃]. All genotypes tested generally showed a decline in biomass with increasing O₃ exposure whether exposure was expressed in terms of [O₃] (i.e. AOT40) or O₃ flux (i.e. POD₀ or POD₂). The response of relative biomass to the metric AOT40 ranged from −0.0015 in Mandalay to −0.0017, −0.0025 and −0.0069 in Q240, CTC4 and Badila respectively. In considering susceptibility to O₃ flux, the genotype-specific O₃ dose-response functions also varied (Table 2, Figs. 2b and A7) from the least susceptible Mandalay, through Q240 and CTC4, to the most susceptible genotype Badila. The pattern of O₃ susceptibility across genotypes was the same when using either no O₃ flux threshold (i.e. POD₀) or a threshold of 2 nmol m^{−2} s^{−1} (i.e. POD₂). Generally we estimated a more negative slope (greater susceptibility) within a genotype when using an increased threshold (Fig. A7). However, in most species the fit was not significantly different between model estimates of relative biomass decline when using a threshold of 0 or 6 nmol m^{−2} s^{−1}, as indicated by an overlap in confidence intervals. Only in Badila did we see an apparent significant increase in susceptibility when using a greater threshold, possibly as a result of the non-linear response in biomass response observed in this genotype (Fig. 2a).

3.2. Morphological impacts of O₃ on sugarcane

Across all sugarcane genotypes, increasing O₃ flux had a statistically significant ($p < 0.01$) and negative impact (beta = −0.15, 95 % CI [−0.24, −0.06], $t_{(32)} = -3.28$) on the LMA of the most recently emerged leaf (i.e. L + 1) (Fig. A8). Similarly, across all genotypes there was a highly significant ($p < 0.001$) and positive impact of O₃ flux on carbon partitioning with a significant impact of O₃ on the ratio of above ground

Table 2

Genotype specific O₃ dose-response functions (±1 S.E.) of sugarcane grown for ~100 days in open top chambers under a range of [O₃] (Fig. 2), using two thresholds for calculating Phytotoxic Ozone Dose (0 and 2 nmol m^{−2} s^{−1}). Relative biomass calculated after setting y-intercept to 1 at POD_y = 0.

POD	Genotype	Total biomass (g)						Relative biomass			p-Value
		Intercept		Slope				Slope			
POD ₀	Badila	388	±	22	−3.91	±	0.73	−0.0101	±	0.0571	<0.01
	CTC4	435	±	14	−1.90	±	0.50	−0.0044	±	0.0011	<0.01
	Mandalay	264	±	11	−0.35	±	0.42	−0.0013	±	0.0016	ns
	Q240	531	±	22	−1.63	±	0.83	−0.0031	±	0.0016	<0.1
POD ₂	Badila	363	±	17	−3.99	±	0.73	−0.0109	±	0.0020	<0.001
	CTC4	423	±	11	−1.96	±	0.51	−0.0046	±	0.0012	<0.01
	Mandalay	263	±	10	−0.33	±	0.40	−0.0013	±	0.0015	ns
	Q240	521	±	17	−1.68	±	0.86	−0.0032	±	0.0016	<0.1

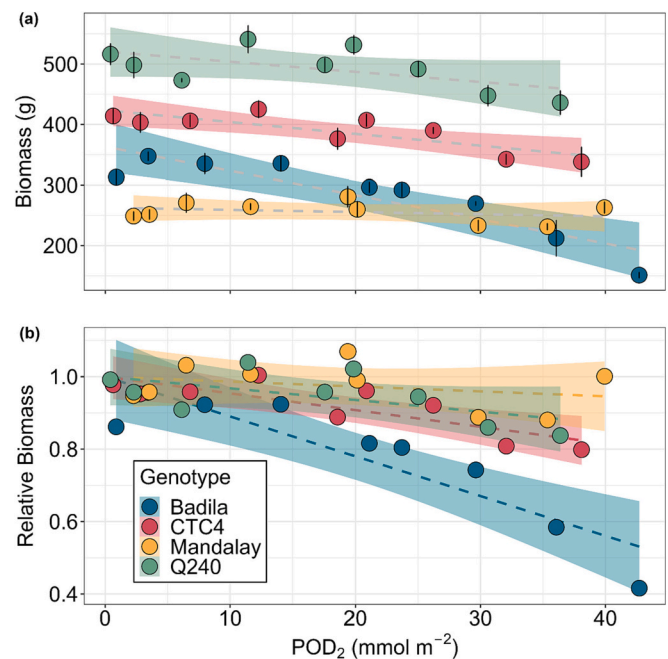


Fig. 2. Ozone dose-response functions of four genetic lines of sugarcane. Values represent average ($n = 4 \pm 1$ S.E.) change in biomass (a) and relative biomass (b) as compared to phytotoxic O₃ dose (POD) above a threshold of 2 nmol m^{−2} s^{−1}.

Table 3

JULES O₃ sensitivity parameter (α) calibrated for four sugarcane scenarios.

Genotype susceptibility	JULES O ₃ sensitivity parameter (α)	
	POD ₀	POD ₂
Low ^a	0.04	0.04
Moderate ^b	0.1	0.1
High ^c	0.25	0.28
Very high ^d	0.9	0.75

^a Calibrated using *S. spontaneum* cv. Mandalay (this study).

^b Calibrated using average of CTC4 and Q240 (this study).

^c Calibrated using *S. officinarum* cv. Badila (this study).

^d Calibrated using average of IACSP94-2094 and IACSP95-5000 (Moura et al., 2018b).

to below ground biomass (beta = 0.03, 95 % CI [0.02, 0.04], $t_{(32)} = 7.75$, Fig. A9).

3.3. Modelling risk of O₃ across south-central Brazil

Our model results highlighted the potential risk of O₃ to sugarcane NPP and, therefore, total production across south-central Brazil (Figs. 3 and A10). All dose-response functions tested showed current O₃

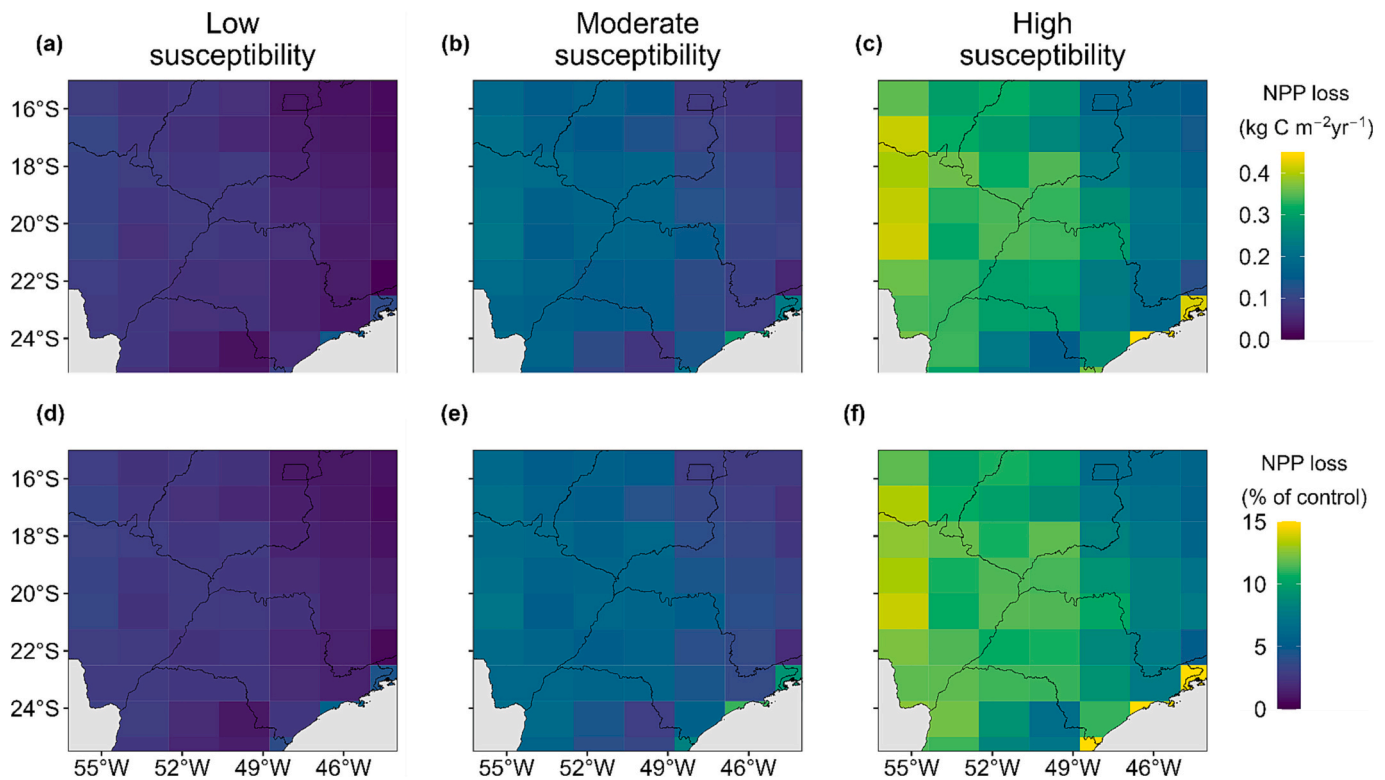


Fig. 3. Modelled risk of present day (i.e. 2010 to 2015) $[O_3]$ on potential sugarcane production across south-central Brazil, expressed as absolute reduction in NPP ($\text{kg C m}^{-2} \text{yr}^{-1}$) and % loss of control NPP (i.e. no O_3). Model calibrated against the range of observed O_3 susceptibility seen in this study examining biomass decline against POD_2 , with low susceptibility (a, d) representing *S. spontaneum* cv. Mandalay, moderate susceptibility (b, e) representing two commercial sugarcane cultivars (CTC4 and Q240) and high susceptibility (c, f) representing *S. officinarum* cv. Badila. Note for clarity cells exceeding upper limit of scale in sub-figures (c) and (f) set to upper limits of $0.45 \text{ kg C m}^{-2} \text{yr}^{-1}$ and 15 % respectively.

exposure would likely lead to a reduction in sugarcane production across the region. The magnitude of this risk was impacted by spatial variation in O_3 exposure, stomatal conductance, and which dose-response function (i.e. low-, moderate- or high- susceptibility) and threshold value (i.e. POD_0 or POD_2) was implemented. Examining the range of potential risk using our moderate susceptibility function (representative of two commercial varieties Q240 and CTC4), we saw the risk to NPP across the region ranging from 0.05 to 0.29 (average 0.14) $\text{kg C m}^{-2} \text{yr}^{-1}$ (Fig. 3a-c) representing between 2.0 and 11.2 % (average 5.1 %) of control model NPP (Fig. 3d-f) when using a threshold of $2 \text{ nmol m}^{-2} \text{s}^{-1}$. The risk of NPP loss increased to between 0.36 and 0.62 (average 0.50) $\text{kg C m}^{-2} \text{yr}^{-1}$ (i.e. 14.7 to 23.6 % (average 17.8 %) of control model NPP) when using no threshold (Fig. A10). For additional context, we also modelled the potential risks on production using previously published data from two other commercial varieties grown in Italy, shown to be

highly susceptible to O_3 (i.e. IACSP94-2094 and IACSP95-5000). Although the comparison of data derived from OTC's and free air O_3 enrichment should be made with caution (Montes et al., 2022), using the observed dose-response for these varieties, current O_3 exposure in south-central Brazil (Fig. A11) would be expected to reduce NPP by on average $0.42 \text{ kg C m}^{-2} \text{yr}^{-1}$ (i.e. 14.9 % of control NPP) using POD_2 or $1.69 \text{ kg C m}^{-2} \text{yr}^{-1}$ (i.e. 61 % of control NPP) using POD_0 (Fig. A11).

In converting spatially explicit maps of the O_3 risk across the landscape to consider the likely impacts on regional production, we took into account where sugarcane production currently occurs. Specifically, we took the fractional cover of sugarcane found across the region in 2020 (Figs. 4 and A12). Depending upon the O_3 susceptibility assumed (i.e. low, moderate or high), we predicted NPP of total sugarcane across the region to be reduced by between 2.5 and 11 % when using POD_2 . However, when examining only the commercial cultivars (i.e. moderate

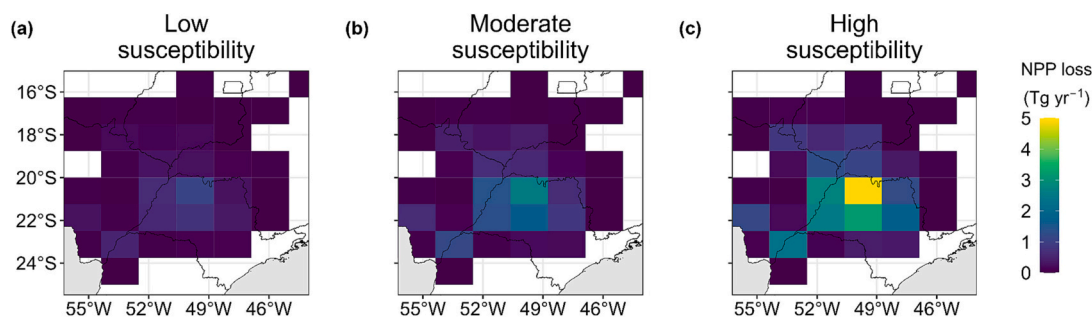


Fig. 4. Predicted total production losses due to present day O_3 damage in sugarcane across south-central Brazil, assuming sugarcane growing locations as per the year 2020 (Souza et al., 2020). Model calibrated using three susceptibilities to O_3 using the flux metric POD_2 . Control model NPP total equals 243 Tg yr^{-1} with predicted total losses in (a) low susceptibility representing *S. spontaneum* cv. Mandalay of 2.5 %, (b) moderate susceptibility representing two commercial sugarcane cultivars (i.e. CTC4 and Q240) of 5.6 %, and (c) high susceptibility representing *S. officinarum* cv. Badila of 11 %.

susceptibility) the likely reduction in NPP increased from 5.6 to 18.3 % of the control scenario NPP when considering POD_0 instead of POD_2 .

4. Discussion

Our results demonstrate that experimental O_3 exposure has a significant and substantial impact on the morphology and biomass accumulation of the globally important C_4 bioenergy crop sugarcane. The decline in relative biomass seen with increasing AOT40 averaged -0.21 % per ppm.h in the two commercial varieties (i.e. CTC4 and Q240) tested making them comparable with other moderately ' O_3 sensitive' crops (Mills et al., 2007) and generally greater than the cotton parameterization previously used in assessment of O_3 impacts on sugarcane production, i.e. -0.1495 % per ppm.h used by Yi et al. (2018) and Chuwah et al. (2015). When making our calculations we assumed a linear decrease in yield with increase in O_3 (concentration or flux), as this is in line with the methodology currently used (CLRTAP et al., 2017). For the varieties Mandalay, CTC4 and Q240 a linear response is appropriate, whereas for Badila the response may be sigmoidal over the range of O_3 exposure used. As this was consistent across the range of flux-thresholds tested, we retained the use of a linear function.

When considering the more biologically relevant metric of O_3 flux under prevailing experimental conditions (i.e. POD_y) we still see a substantial difference in susceptibility of genotypes tested (Table 2, Fig. A7), highlighting the likely role that fundamental plant traits play in shaping observed O_3 responses. In our novel dataset, we observed a trend in O_3 susceptibility across genotypes similar to the decline of net photosynthesis reported by Grantz et al. (2012), with values ranging from *S. spontaneum* (low susceptibility) through commercial hybrids (moderate susceptibility) to *S. officinarum* (high susceptibility). In comparing the O_3 susceptibility reported here to the only comparable O_3 -flux data available for sugarcane, an average dose-response at POD_2 of -0.03645 seen in above ground biomass of genotypes IACSP95-5000 and IACSP94-2094 (Moura et al., 2018b), we found all genotypes tested here to be generally less susceptible (Table 2). Using the 'very high' susceptibility observed in Moura et al. (2018b) to parameterize JULES resulted in a substantial increase in modelled risk to production across south central Brazil (c.f. Figs. 3 and A11). Although this is likely due to the difference in cultivar susceptibility often seen in C_4 crops (Li et al., 2022), differences between the experimental design and analysis i.e. repeated-treatments in Moura et al. (2018b), and gradient-designs (this study), as well as fundamental differences between responses seen in OTC and free air O_3 enrichment studies (Montes et al., 2022) likely play a role. Further work to identify drivers of O_3 susceptibility in relevant production genotypes is needed to assess the accuracy of any future model parameterizations.

When using our observed O_3 susceptibility to parameterize the dynamic vegetation model JULES, we found that current $[O_3]$ in south-central Brazil is likely contributing to a substantial yield gap (i.e. difference between potential and observed yields) seen in sugarcane across the region. Our control model with sugarcane not exposed to O_3 predicted potential NPP of up to $3.1 \text{ kg C m}^{-2} \text{ yr}^{-1}$, equating to a yield of $\sim 138 \text{ Mg ha}^{-1}$. The potential risk of current O_3 on production of commercial cultivars (moderate susceptibility in this study) across south-central Brazil equated to a yield gap of between 2.2 and 13.0 Mg ha^{-1} (average 6.3 Mg ha^{-1}) when using POD_2 , and between 16.1 and 27.8 Mg ha^{-1} (average 22.4 Mg ha^{-1}) using POD_0 . This resulted in a prediction of water-limited yield (Y_w), while accounting for O_3 impacts, in a range comparable to that derived from calibrated crop modelling estimates at between 93.5 and 132 Mg ha^{-1} (average 109 Mg ha^{-1}) in south-central Brazil (Dias and Sentelhas, 2018). Calibrated crop models do not currently account for the impacts of O_3 , however by their nature they implicitly account for O_3 damage in the data used to parameterize them. While observed yields in the region are currently much lower than even water-limited potential at between 38.5 and 90.4 Mg ha^{-1} (average

78 Mg ha^{-1}) (Dias and Sentelhas, 2018), our finding suggests that O_3 is likely contributing to the substantial yield gap observed in Brazil (Dias and Sentelhas, 2018; Marin et al., 2016) and that, even if improvements to growing conditions and management practices are made, a yield gap will likely remain. Indeed, the adoption of improved irrigation (currently only a small fraction of total production area) may lead to a greater O_3 penalty via the removal of stomatal exclusion of O_3 through reduced g_s during periods of drought (Gao et al., 2017; Harmens et al., 2019), which are often associated with poor air quality (Targino et al., 2019).

Given the range of genetic material used in modern sugarcane breeding programs, there is the potential for selecting tolerant commercial cultivars for regions of particularly high O_3 risk. However, there is also the more general need to consider O_3 sensitivity in the screening of new cultivars to avoid inadvertently developing 'high yield' varieties that are more susceptible to O_3 (Osborne et al., 2016). We suggest that cultivar O_3 -susceptibility, the possible counter-intuitive impacts of irrigation, and predictions of future air quality across Brazil all need to be considered to ensure the sustainable expansion of the industry (Rossetto et al., 2022) within Sugarcane Agroecological Zoning (da Silva et al., 2021).

The advantages of a flux based approach to assessing O_3 susceptibility have been well established (Pleijel et al., 2022) and has been used here to translate observed susceptibility in sugarcane to a landscape-scale model that has an ability to predict dynamic g_s . In plotting the relationship between ambient O_3 concentration and modelled stomatal flux of O_3 (Fig. 5) across south-central Brazil we show how stomatal exclusion – the limitation of O_3 flux due to stomatal closure – results in a broad range of O_3 fluxes calculated for any given level of $[O_3]$ exposure. This avoidance of O_3 via stomatal exclusion would not be reflected in concentration metrics such as AOT40 or SUM60 used to characterize O_3 exposure.

When calculating POD_y , the use of a threshold value (e.g. 1, 2 or $6 \text{ nmol m}^{-2} \text{ s}^{-1}$) is often expounded to account for the plant's intrinsic antioxidant capacity or indeed the commonly observed hormetic response of plants to increasing $[O_3]$ (Agathokleous et al., 2019). Across our control model run, the consideration of an instantaneous threshold of $2 \text{ nmol m}^{-2} \text{ s}^{-1}$ (equating to $[O_3] \sim 10 \text{ ppb}$ under non limiting g_s) reduces the sum of accumulated flux by ~ 43 % as compared to not having a threshold. The inclusion of a flux threshold acts to shorten the daily period over which O_3 damage occurs (Fig. 5b). Lower g_s in the morning and late afternoon, combined with lower $[O_3]$ during these periods, leads to O_3 fluxes that fall below the $2 \text{ nmol m}^{-2} \text{ s}^{-1}$, despite midday O_3 fluxes that are often above this threshold. The influence of this threshold value can also be compounded over time when using dynamic vegetation models as is shown when modelling annualized production losses. Specifically, when considering no threshold (POD_0 , Fig. A12), yield losses were predicted to be approximately three times larger in south-central Brazil compared to when using POD_2 (Fig. 4). Care is therefore needed to ensure the biological relevance of metrics applied to ensure an accurate representation of potential O_3 damage.

The O_3 damage scheme used in global DGVM's such as JULES is by necessity simplistic, representing productivity decreases via an instantaneous reduction in both A_{net} and concomitant g_s . It therefore does not account for the potential decoupling of photosynthetic capacity and g_s under high $[O_3]$ (Cernusak et al., 2021; Li et al., 2021), the observed acceleration of leaf senescence under high $[O_3]$ (Gielen et al., 2007), nor the cumulative impacts of progressive and increasing root biomass decline under high $[O_3]$ (Fig. A9, see also Grantz and Vu (2009)). For perennial crops such as sugarcane, often grown with multiple ratoon cycles, it is reasonable to assume a cumulative change in partitioning might translate into further reductions in productivity over, for example, a 5-year cycle.

The integration of more biologically realistic O_3 damage schemes into dedicated crop models (i.e. DSSAT/CANEGRO, APSIM-Sugarcane) has previously been identified as a bottleneck to the development of

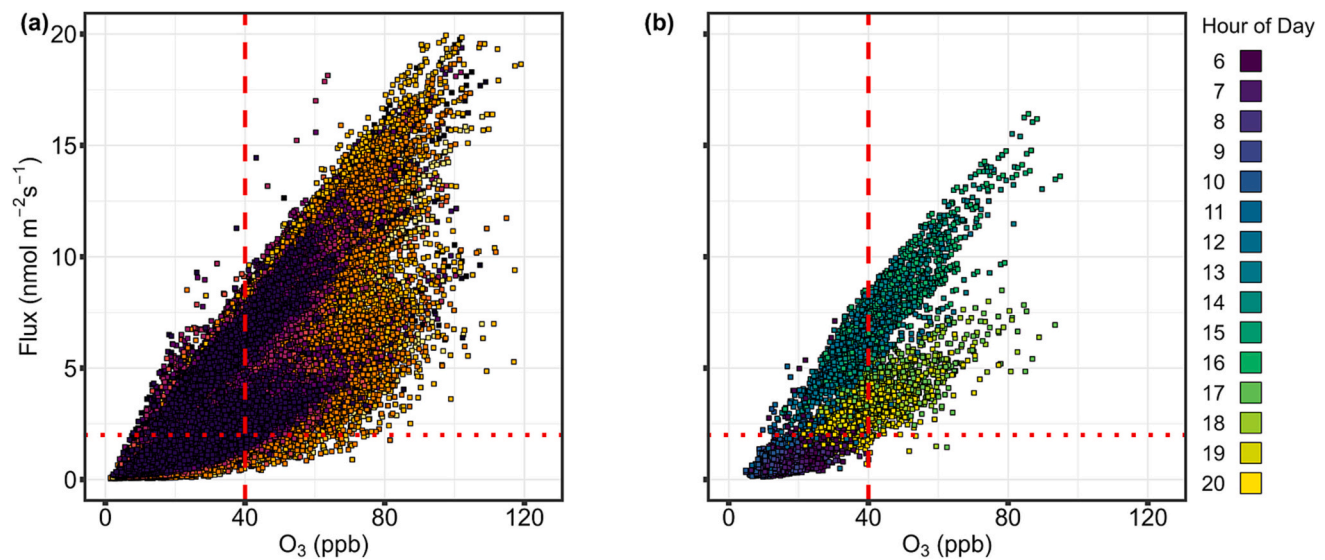


Fig. 5. Daytime (06:00 to 20:00) hourly O_3 exposure and calculated stomatal fluxes of O_3 into sugarcane modelled using JULES across south-central Brazil. Model outputs represent only control scenario for clarity (given negative feedback of O_3 damage on g_s in current O_3 scheme as used in JULES). (a) shows all terrestrial grid cells with grid cell identity represented by different colors, in (b) results of a single grid cell ($-20.625, 310.3125$, chosen as it contains the highest fraction of land cover dedicated to sugarcane production in south-central Brazil) with hour represented by color. Thresholds of fluxes equal to $2 \text{ nmol m}^{-2} \text{ s}^{-1}$ (dotted red line) and concentration equal to 40 ppb (dashed red line) indicated.

accurate predictions on future O_3 yield impacts (Emberson et al., 2018). However, despite the extensive resources marshalled through international efforts such as the AgMIP program (<https://agmip.org/4309-2/>) we are only now beginning to see the inclusion of O_3 damage in this fashion into the modelling of highly studied temperate crops such as winter wheat (Feng et al., 2022). Our results highlight the likely impact of current O_3 on sugarcane production, as well as the need to account for genotypic variation in functional traits that can determine O_3 susceptibility (Wedow et al., 2021). The development of modelling-frameworks that can account for this variation (both between cultivars and during ontogenetic development), and translate impacts of NPP decline into changes in sugarcane quality (i.e. sucrose and fibre content) may provide more accurate estimates of the economic costs of O_3 . This will also allow insights into how potential O_3 mediation strategies, such as farm management practice and the use of new cultivar selection, can be used to close the O_3 yield gap (Emberson et al., 2018).

CRedit authorship contribution statement

Alexander W. Cheesman: Conceptualization, Methodology, Formal analysis, Investigation, Writing – original draft, Visualization, Supervision, Project administration, Funding acquisition. **Flossie Brown:** Methodology, Investigation, Formal analysis, Writing – review & editing. **Nahid Farha:** Investigation. **Thais M. Rosan:** Resources. **Gerd Folberth:** Writing – review & editing, Funding acquisition. **Felicity Hayes:** Conceptualization, Writing – review & editing, Funding acquisition. **Barbara B. Moura:** Resources, Writing – review & editing, Funding acquisition. **Elena Paoletti:** Resources, Writing – review & editing, Funding acquisition. **Yasutomo Hoshika:** Resources, Writing – review & editing, Funding acquisition. **Colin P. Osborne:** Writing – review & editing, Funding acquisition. **Lucas A. Cernusak:** Resources, Writing – review & editing, Funding acquisition. **Rafael V. Ribeiro:** Conceptualization, Writing – review & editing, Funding acquisition. **Stephen Sitch:** Conceptualization, Writing – review & editing, Supervision, Funding acquisition.

Declaration of competing interest

The authors declare that they have no known competing financial

interests or personal relationships that could have appeared to influence the work reported in this paper.

Data availability

Data will be made available on request.

Acknowledgments

This research was funded through UKRI NERC- Brazilian FAPESP combined funding schemes (NE/V008498/1 and FAPESP Grant #2020/04652-6) and Bilateral Agreement of CNR and FAPESP 2022-2023 (B85F22000090005) ‘Environmental impacts of ozone and climatic changes on major Brazilian crops (sugarcane and coffee cultivars)’. We would like to thank the Centro de Tecnologia Canavieira (CTC) and Sugar Research Australia (SRA) for licencing access to germplasm collections held by SRA and to Dr. Jason Eglinton and Dr. Felicity Atkin for advice in the collection and propagation of sugarcane. RVR is a fellow of the National Council for Scientific and Technological Development (CNPq, Brazil). GAF wishes to acknowledge support by the Met Office Hadley Centre Climate Programme funded by BEIS and Defra (GA01101). The authors thank Murilo Vianna on sugarcane parameterizations in the JULES model and Rebecca Oliver for advice on utilising the most up-to-date O_3 -damage scheme in JULES. FB was funded by the NERC GW4+ DTP—award number NE/S007504/1—and the Met Office on a CASE studentship.

Appendix A. Supplementary data

Supplementary data to this article can be found online at <https://doi.org/10.1016/j.scitotenv.2023.166817>.

References

- Agathokleous, E., Saitanis, C.J., 2020. Plant susceptibility to ozone: a tower of Babel? *Sci. Total Environ.* 703, 134962.
- Agathokleous, E., Belz, R.G., Calatayud, V., De Marco, A., Hoshika, Y., Kitao, M., et al., 2019. Predicting the effect of ozone on vegetation via linear non-threshold (LNT), threshold and hormetic dose-response models predicting the effect of ozone on vegetation via linear non-threshold (LNT), threshold and hormetic dose-response models. *Sci. Total Environ.* 649, 61–74.

- Ainsworth, E.A., 2017. Understanding and improving global crop response to ozone pollution. *Plant J.* 90, 886–897.
- ALESP, 2002. In: Assembleia Legislativa do Estado de São Paulo B (Ed.), Lei 11,241, de 19 de setembro de 2002- Dispõe sobre a eliminação gradativa da queima da palha da cana-de-açúcar e dá providências correlatas.
- Basnayake, J., Jackson, P.A., Inman-Bamber, N.G., Lakshmanan, P., 2015. Sugarcane for water-limited environments. Variation in stomatal conductance and its genetic correlation with crop productivity. *J. Exp. Bot.* 66, 3945–3958.
- Best, M.J., Pryor, M., Clark, D.B., Rooney, G.G., Essery, R.L.H., Ménard, C.B., et al., 2011. The Joint UK Land Environment Simulator (JULES), model description – part 1: energy and water fluxes. *Geosci. Model Dev.* 4, 677–699.
- Boaretto, L.F., Carvalho, G., Borgo, L., Creste, S., Landell, M.G.A., Mazzafera, P., et al., 2014. Water stress reveals differential antioxidant responses of tolerant and non-tolerant sugarcane genotypes. *Plant Physiol. Biochem.* 74, 165–175.
- Braga Junior, RldC, Landell, MgdA, da Silva, D.N., Bidóia, M.A.P., da Silva, T.N., da Silva, V.H.P., et al., 2021. Censo Varietal IAC de cana-de-açúcar no Brasil-Safra 2018/2019 e na região Centro-Sul-Safra 2019/20. Instituto Agronômico, Campinas.
- Brown, F., Folberth, G.A., Sitch, S., Bauer, S., Bauters, M., Boeckx, P., et al., 2022. The ozone–climate penalty over South America and Africa by 2100. *EGU sphere* 22, 12331–12352.
- Cernusak, L.A., Farha, M.N., Cheesman, A.W., 2021. Understanding how ozone impacts plant water-use efficiency. *Tree Physiol.* 41, 2229–2233.
- Chuwah, C., van Noije, T., van Vuuren, D.P., Stehfest, E., Hazeleger, W., 2015. Global impacts of surface ozone changes on crop yields and land use. *Atmos. Environ.* 106, 11–23.
- Clark, D.B., Mercado, L.M., Sitch, S., Jones, C.D., Gedney, N., Best, M.J., et al., 2011. The Joint UK Land Environment Simulator (JULES), model description – part 2: carbon fluxes and vegetation dynamics. *Geosci. Model Dev.* 4, 701–722.
- CLRTAP, Mills, G., Harmens, H., Hayes, F., Pleijel, H., Büker, P., et al., 2017. Mapping critical levels for vegetation. In: Revised Chapter 3 of the Manual on Methodologies and Criteria for Modelling and Mapping Critical Loads and Levels and Air Pollution Effects, Risks and Trends.
- Dias, H.B., Sentelhas, P.C., 2018. Sugarcane yield gap analysis in Brazil – a multi-model approach for determining magnitudes and causes. *Sci. Total Environ.* 637–638, 1127–1136.
- Doherty, R.M., 2015. Ozone pollution from near and far. *Nat. Geosci.* 8, 664–665.
- Emberson, L.D., 2020. Effects of ozone on agriculture, forests and grasslands. *Philos. Transact. A Math. Phys. Eng. Sci.* 378, 20190327.
- Emberson, L.D., Ashmore, M.R., Cambridge, H.M., Simpson, D., Tuovinen, J.P., 2000. Modelling stomatal ozone flux across Europe. *Environ. Pollut.* 109, 403–413.
- Emberson, L.D., Pleijel, H., Ainsworth, E.A., van den Berg, M., Ren, W., Osborne, S., et al., 2018. Ozone effects on crops and consideration in crop models. *Eur. J. Agron.* 100, 19–34.
- EPE, 2023. Matriz energética e elétrica. Empresa de Pesquisa Energética, Brazil.
- FAOSTAT, 2021. Statistical Database. Food and Agriculture Organization of the United Nations, Rome.
- Feng, Y.R., Nguyen, T.H., Alam, M.S., Emberson, L., Gaiser, T., Ewert, F., et al., 2022. Identifying and modelling key physiological traits that confer tolerance or sensitivity to ozone in winter wheat. *Environ. Pollut.* 304, 119251.
- Folberth, G.A., Butler, T.M., Collins, W.J., Rumbold, S.T., 2015. Megacities and climate change – a brief overview. *Environ. Pollut.* 203, 235–242.
- Gao, F., Catalayud, V., Paoletti, E., Hoshika, Y., Feng, Z.Z., 2017. Water stress mitigates the negative effects of ozone on photosynthesis and biomass in poplar plants. *Environ. Pollut.* 230, 268–279.
- Gielen, B., Löw, M., Deckmyn, G., Metzger, U., Franck, F., Heerd, C., et al., 2007. Chronic ozone exposure affects leaf senescence of adult beech trees: a chlorophyll fluorescence approach. *J. Exp. Bot.* 58, 785–795.
- Granier, C., Müller, J.-F., Brousseau, G., 2000. The impact of biomass burning on the global budget of ozone and ozone precursors. In: Innes, J.L., Beniston, M., Verstraete, M.M. (Eds.), *Biomass Burning and its Inter-relationships With the Climate System*. Springer, Netherlands, Dordrecht, pp. 69–85.
- Grantz, D.A., Vu, H.B., 2009. O₃ sensitivity in a potential C₄ bioenergy crop: sugarcane in California. *Crop Sci.* 49, 643–650.
- Grantz, D.A., Vu, H.B., Tew, T.L., Veremis, J.C., 2012. Sensitivity of gas exchange parameters to ozone in diverse C₄ sugarcane hybrids. *Crop Sci.* 52, 1270–1280.
- Harmens, H., Hayes, F., Sharps, K., Radbourne, A., Mills, G., 2019. Can reduced irrigation mitigate ozone impacts on an ozone-sensitive African wheat variety? *Plants* 8, 220.
- Harper, A.B., Cox, P.M., Friedlingstein, P., Wiltshire, A.J., Jones, C.D., Sitch, S., et al., 2016. Improved representation of plant functional types and physiology in the Joint UK Land Environment Simulator (JULES v4.2) using plant trait information. *Geosci. Model Dev.* 9, 2415–2440.
- Harper, A.B., Williams, K.E., McGuire, P.C., Rojas, M.C.D., Hemming, D., Verhoef, A., et al., 2021. Improvement of modeling plant responses to low soil moisture in JULESv4.9 and evaluation against flux tower measurements. *Geosci. Model Dev.* 14, 3269–3294.
- Harris, I., Osborn, T.J., Jones, P., Lister, D., 2020. Version 4 of the CRU TS monthly high-resolution gridded multivariate climate dataset. *Sci. Data* 7, 109.
- Hayes, F., Sharps, K., Harmens, H., Roberts, I., Mills, G., 2020. Tropospheric ozone pollution reduces the yield of African crops. *J. Agron. Crop Sci.* 206, 214–228.
- Hewitt, C.N., MacKenzie, A.R., Di Carlo, P., Di Marco, C.F., Dorsey, J.R., Evans, M., et al., 2009. Nitrogen management is essential to prevent tropical oil palm plantations from causing ground-level ozone pollution. *Proc. Natl. Acad. Sci.* 106, 18447–18451.
- Huntingford, C., Zelazowski, P., Galbraith, D., Mercado, L.M., Sitch, S., Fisher, R., et al., 2013. Simulated resilience of tropical rainforests to CO₂-induced climate change. *Nat. Geosci.* 6, 268–273.
- Huntingford, C., Atkin, O.K., Martinez-de la Torre, A., Mercado, L.M., Heskel, M.A., Harper, A.B., et al., 2017. Implications of improved representations of plant respiration in a changing climate. *Nat. Commun.* 8, 1602.
- Huntingford, C., Burke, E.J., Jones, C.D., Jeffers, E.S., Wiltshire, A.J., 2022. Nitrogen cycle impacts on CO₂ fertilisation and climate forcing of land carbon stores. *Environ. Res. Lett.* 17, 044072.
- IBGE, 2023. Produção agropecuária. Instituto Brasileiro de Geografia e Estatística, Brazil.
- Jarvis, P.G., 1976. Interpretation of variations in leaf-water potential and stomatal conductance found in canopies in field. *Philos. Trans. R. Soc. Lond., B, Biol. Sci.* 273, 593–610.
- Kobayashi, S., Ota, Y., Harada, Y., Ebata, A., Moriwa, M., Onoda, H., et al., 2015. The JRA-55 reanalysis: general specifications and basic characteristics. *J. Meteorol. Soc. Jpn.* 93, 5–48.
- Kreyling, J., Schweiger, A.H., Bahn, M., Ineson, P., Migliavacca, M., Morel-Journel, T., et al., 2018. To replicate, or not to replicate – that is the question: how to tackle nonlinear responses in ecological experiments. *Ecol. Lett.* 21, 1629–1638.
- Lelieveld, J., Evans, J.S., Fnais, M., Giannadaki, D., Pozzer, A., 2015. The contribution of outdoor air pollution sources to premature mortality on a global scale. *Nature* 525, 367–371.
- Leung, F., Sitch, S., Tai, A.P.K., Wiltshire, A.J., Gornall, J.L., Folberth, G.A., et al., 2022. CO₂ fertilization of crops offsets yield losses due to future surface ozone damage and climate change. *Environ. Res. Lett.* 17, 074007.
- Li, P., Feng, Z., Shang, B., Uddling, J., 2021. Combining carbon and oxygen isotopic signatures to identify ozone-induced declines in tree water-use efficiency. *Tree Physiol.* 41, 2234–2244.
- Li, S., Moller, C.A., Mitchell, N.G., Lee, D., Sacks, E.J., Ainsworth, E.A., 2022. Testing unified theories for ozone response in C₄ species. *Glob. Chang. Biol.* 28, 3379–3393.
- Marin, F.R., Thorburn, P.J., Nassif, D.S.P., Costa, L.G., 2015. Sugarcane model intercomparison: structural differences and uncertainties under current and potential future climates. *Environ. Model Softw.* 72, 372–386.
- Marin, F.R., Martha Jr., G.B., Cassman, K.G., Grassini, P., 2016. Prospects for increasing sugarcane and bioethanol production on existing crop area in Brazil. *BioScience* 66, 307–316.
- Medlyn, B.E., Duursma, R.A., Eamus, D., Ellsworth, D.S., Prentice, I.C., Barton, C.V.M., et al., 2011. Reconciling the optimal and empirical approaches to modelling stomatal conductance. *Glob. Chang. Biol.* 17, 2134–2144.
- Mercado, L.M., Bellouin, N., Sitch, S., Boucher, O., Huntingford, C., Wild, M., et al., 2009. Impact of changes in diffuse radiation on the global land carbon sink. *Nature* 458, 1014–1017.
- Mills, G., Buse, A., Gimeno, B., Bermejo, V., Holland, M., Emberson, L., et al., 2007. A synthesis of AOT40-based response functions and critical levels of ozone for agricultural and horticultural crops. *Atmos. Environ.* 41, 2630–2643.
- Mills, G., Pleijel, H., Malley, C.S., Sinha, B., Cooper, O.R., Schultz, M.G., et al., 2018a. Tropospheric ozone assessment report: present-day tropospheric ozone distribution and trends relevant to vegetation. *Elementa* 6, 46.
- Mills, G., Sharps, K., Simpson, D., Pleijel, H., Frei, M., Burkey, K., et al., 2018b. Closing the global ozone yield gap: quantification and cobenefits for multistress tolerance. *Glob. Chang. Biol.* 24, 4869–4893.
- Montes, C.M., Demler, H.J., Li, S., Martin, D.G., Ainsworth, E.A., 2022. Approaches to investigate crop responses to ozone pollution: from O₃-FACE to satellite-enabled modeling. *Plant J.* 109, 432–446.
- Moore, P.H., Paterson, A.H., Tew, T., 2014. Sugarcane: the crop, the plant and domestication. In: Moore, P.H., Botha, F.C. (Eds.), *Sugarcane: Physiology, Biochemistry and Functional Biology*. John Wiley & Sons, pp. 1–18.
- Moura, B.B., Alves, E.S., Marabesi, M.A., de Souza, S.R., Schaub, M., Vollenweider, P., 2018a. Ozone affects leaf physiology and causes injury to foliage of native tree species from the tropical Atlantic Forest of southern Brazil. *Sci. Total Environ.* 610, 912–925.
- Moura, B.B., Hoshika, Y., Ribeiro, R.V., Paoletti, E., 2018b. Exposure- and flux-based assessment of ozone risk to sugarcane plants. *Atmos. Environ.* 176, 252–260.
- Moura, B.B., Hoshika, Y., Silveira, N.M., Marcos, F.C.C., Machado, E.C., Paoletti, E., et al., 2018c. Physiological and biochemical responses of two sugarcane genotypes growing under free-air ozone exposure. *Environ. Exp. Bot.* 153, 72–79.
- Natarajan, S., Basnayake, J., Lakshmanan, P., Fukai, S., 2021. Genotypic variation in intrinsic transpiration efficiency correlates with sugarcane yield under rainfed and irrigated field conditions. *Physiol. Plant.* 172, 976–989.
- Ogura, A.P., da Silva, A.C., Castro, G.B., Espindola, E.L.G., da Silva, A.L., 2022. An overview of the sugarcane expansion in the state of São Paulo (Brazil) over the last two decades and its environmental impacts. *Sustain. Prod. Consum.* 32, 66–75.
- Oliver, R.J., Mercado, L.M., Sitch, S., Simpson, D., Medlyn, B.E., Lin, Y.S., et al., 2018. Large but decreasing effect of ozone on the European carbon sink. *Biogeosciences* 15, 4245–4269.
- Osborne, S.A., Mills, G., Hayes, F., Ainsworth, E.A., Buker, P., Emberson, L., 2016. Has the sensitivity of soybean cultivars to ozone pollution increased with time? An analysis of published dose-response data. *Glob. Chang. Biol.* 22, 3097–3111.
- Pleijel, H., Danielsson, H., Broberg, M.C., 2022. Benefits of the Phytotoxic Ozone Dose (POD) index in dose-response functions for wheat yield loss. *Atmos. Environ.* 268, 118797.
- R Core Team, 2022. R: A Language and Environment for Statistical Computing. R Foundation for Statistical Computing, Vienna, Austria.
- Rao, X.L., Dixon, R.A., 2016. The differences between NAD-ME and NADP-ME subtypes of C₄ photosynthesis: more than decarboxylating enzymes. *Front. Plant Sci.* 7, 1525.
- Rap, A., Scott, C.E., Reddington, C.L., Mercado, L., Ellis, R.J., Garraway, S., et al., 2018. Enhanced global primary production by biogenic aerosol via diffuse radiation fertilization. *Nat. Geosci.* 11, 640–644.

- Richards, B.L., Middleton, J.T., Hewitt, W.B., 1958. Air pollution with relation to agronomic crops: V. Oxidant stipple of grape. *Agron. J.* 50, 559–561.
- Rossetto, R., Ramos, N.P., Pires, R.C.D., Xavier, M.A., Cantarella, H., Landell, M.G.D., 2022. Sustainability in sugarcane supply chain in Brazil: issues and way forward. *Sugar Tech* 24, 941–966.
- Sage, R.F., Peixoto, M.M., Sage, T.L., 2014. Photosynthesis in sugarcane. In: Moore, P.H., Botha, F.C. (Eds.), *Sugarcane: Physiology, Biochemistry and Functional Biology*. John Wiley & Sons, pp. 121–154.
- Schuch, D., de Freitas, E.D., Espinosa, S.I., Martins, L.D., Carvalho, V.S.B., Ramin, B.F., et al., 2019. A two decades study on ozone variability and trend over the main urban areas of the São Paulo state, Brazil. *Environ. Sci. Pollut. Res.* 26, 31699–31716.
- da Silva, G.J., Berg, E.C., Calijuri, M.L., dos Santos, V.J., Lorentz, J.F., Alves, S.D., 2021. Aptitude of areas planned for sugarcane cultivation expansion in the state of São Paulo, Brazil: a study based on climate change effects. *Agric. Ecosyst. Environ.* 305, 107164.
- Sitch, S., Cox, P.M., Collins, W.J., Huntingford, C., 2007. Indirect radiative forcing of climate change through ozone effects on the land-carbon sink. *Nature* 448, 791–794.
- Souza, C.M., Shimbo, J., Rosa, M.R., Parente, L.L., Alencar, A., BFT, Rudorff, et al., 2020. Reconstructing three decades of land use and land cover changes in Brazilian biomes with Landsat archive and earth engine. *Remote Sens.* 12, 2735.
- Spera, S., 2017. Agricultural intensification can preserve the Brazilian Cerrado: applying lessons from Mato Grosso and Goiás to Brazil's last agricultural frontier. *Trop. Conserv. Sci.* 10, 7.
- Squizzato, R., Nogueira, T., Martins, L.D., Martins, J.A., Astolfo, R., Machado, C.B., et al., 2021. Beyond megacities: tracking air pollution from urban areas and biomass burning in Brazil. *npj Clim. Atmos. Sci.* 4, 17.
- Tai, A.P.K., Martin, M.V., Heald, C.L., 2014. Threat to future global food security from climate change and ozone air pollution. *Nat. Clim. Chang.* 4, 817–821.
- Targino, A.C., Harrison, R.M., Krecl, P., Glantz, P., de Lima, C.H., Beddows, D., 2019. Surface ozone climatology of South Eastern Brazil and the impact of biomass burning events. *J. Environ. Manag.* 252, 109645.
- Urban, R.C., Alves, C.A., Allen, A.G., Cardoso, A.A., Campos, M.L.A.M., 2016. Organic aerosols in a Brazilian agro-industrial area: speciation and impact of biomass burning. *Atmos. Res.* 169, 271–279.
- Vandenbergh, L.P.S., Valladares-Diestra, K.K., Bittencourt, G.A., Torres, L.A.Z., Vieira, S., Karp, S.G., et al., 2022. Beyond sugar and ethanol: the future of sugarcane biorefineries in Brazil. *Renew. Sust. Energ. Rev.* 167, 112721.
- Vianna, M.S., Williams, K.W., Littleton, E.W., Cabral, O., Cerri, C.E.P., Jong, De, van Lier, Q., et al., 2022. Improving the representation of sugarcane crop in the Joint UK Land Environment Simulator (JULES) model for climate impact assessment. *GCB Bioenergy* 14, 1097–1116.
- Volin, J.C., Reich, P.B., Givnish, T.J., 1998. Elevated carbon dioxide ameliorates the effects of ozone on photosynthesis and growth: species respond similarly regardless of photosynthetic pathway or plant functional group. *New Phytol.* 138, 315–325.
- Wedow, J.M., Ainsworth, E.A., Li, S., 2021. Plant biochemistry influences tropospheric ozone formation, destruction, deposition, and response. *Trends Biochem. Sci.* 46, 992–1002.
- Yi, F., McCarl, B.A., Zhou, X., Jiang, F., 2018. Damages of surface ozone: evidence from agricultural sector in China. *Environ. Res. Lett.* 13, 034019.
- Zalles, V., Hansen, M.C., Potapov, P.V., Stehman, S.V., Tyukavina, A., Pickens, A., et al., 2019. Near doubling of Brazil's intensive row crop area since 2000. *Proc. Natl. Acad. Sci. U. S. A.* 116, 428–435.
- Zheng, Y., Luciano, A.C.D., Dong, J., Yuan, W.P., 2022. High-resolution map of sugarcane cultivation in Brazil using a phenology-based method. *Earth Syst. Sci. Data* 14, 2065–2080.